



Published in final edited form as:

Adv Cell Gene Ther. 2018 September ; 1(2): . doi:10.1002/acg2.11.

CAR T cells targeting $\alpha_v\beta_3$ integrin are effective against advanced cancer in preclinical models

Lars Wallstabe¹, Andreas Maded¹, Silke Frenz¹, Hermann Einsele¹, Christoph Rader², and Michael Hudecek¹

¹Medizinische Klinik und Poliklinik II, Universitätsklinikum Würzburg, Würzburg, Germany

²Department of Immunology and Microbiology, The Scripps Research Institute, Jupiter, Florida, USA

Abstract

Objective: Integrins are heterodimeric receptors that convey cell-to-cell and cell-to-matrix interactions. Integrin $\alpha_v\beta_3$ is expressed in several tumour entities including melanoma, glioblastoma, breast, pancreatic and prostate cancer, where it promotes tumour cell survival and metastasis. Here, we generated $\alpha_v\beta_3$ -specific chimeric antigen receptor (CAR) T-cells and analysed their antitumour function in pre-clinical models *in vitro* and *in vivo*.

Methods: $\alpha_v\beta_3$ -CARs comprising a super-humanised hLM609 targeting domain with either high or low affinity (hLM609v7, $K_d = 3$ nM vs. hLM609v11, $K_d = 160$ nM) and equipped with either a long or a short IgG4-Fc extracellular spacer (229 vs. 12 amino acids) were expressed in CD8⁺ and CD4⁺ T-cells through lentiviral transduction.

Results: $\alpha_v\beta_3$ -CAR T-cells eliminated $\alpha_v\beta_3$ -positive tumour cells rapidly and specifically, produced IFN- γ and IL-2 (CD4⁺ > CD8⁺) and exhibited productive proliferation. *In vitro*, we observed the strongest reactivity with the higher-affinity hLM609v7 $\alpha_v\beta_3$ -CAR in the short spacer configuration, consistent with the tumour membrane-distal localization of the hLM609 epitope. In a murine xenograft model of metastatic A-375 melanoma, the strongest antitumour effect was mediated by the lower-affinity hLM609v11 $\alpha_v\beta_3$ -CAR. Notably, a single administration of hLM609v11 $\alpha_v\beta_3$ -CAR T-cells was able to induce complete elimination of melanoma lesions, leading to long-term tumour-free survival.

Conclusions: These data establish $\alpha_v\beta_3$ integrin as a novel target for CAR T-cell immunotherapy, and affirm our previous notion that binding domain affinity and spacer length can be calibrated to augment CAR reactivity.

Michael Hudecek, Medizinische Klinik und Poliklinik II, Universitätsklinikum Würzburg, Würzburg, Germany. Hudecek_M@ukw.de.

Conflict of Interest Statement

M.H. is co-inventor on a patent application (PCT/US2013/055862) related to CAR spacer design that has been filed by the Fred Hutchinson Cancer Research Center (Seattle, WA) and licensed by JUNO Therapeutics, Inc.. C.R. is co-inventor of U.S. Patent 7,087,409 that claims the humanised LM609 variants and is owned by The Scripps Research Institute (La Jolla, CA).

Ethics Statement

The authors confirm that the ethical policies of the journal, as noted on the journal's author guidelines page, have been adhered to and the appropriate ethical review committee approval has been received.

Clinical implications: $\alpha_v\beta_3$ -CAR T-cells have therapeutic potential in several prevalent solid tumours, including melanoma and triple-negative breast cancer.

Keywords

cancer immunotherapy; chimeric antigen receptor (CAR); integrin $\alpha_v\beta_3$; hLM609; melanoma

Introduction

Integrins are heterodimeric cell surface receptors expressed by all nucleated cells and involved in adhesion and signalling processes between cells and their microenvironment. They are formed by non-covalent association of one α - and one β -subunit¹. Upon binding of their respective ligands, integrins recruit large signalling complexes to their cytoplasmic domain and transmit information about the cell's functional state to the microenvironment by modulating the binding affinity to their ligands through conformational changes². Because integrins influence tumour cell migration, invasion, proliferation and survival, they are being pursued as molecular and immunologic targets in cancer therapy³. Integrin $\alpha_v\beta_3$, also known as vitronectin receptor, is one of the best-studied integrins in cancer research. It primarily interacts with ligand proteins containing an RGD-motif and can increase tumour cell survival^{4,5}. Several mechanisms have been identified that link expression of integrin $\alpha_v\beta_3$ on tumour cells to increased metastatic spread^{6,7}. First, the activated form of integrin $\alpha_v\beta_3$ enables binding to platelets, which protects tumour cells from shear stress and enhances their adhesion to blood vessels^{8,9}. Second, recruitment and activation of the tyrosine kinase c-Src by the cytoplasmic tail of the β_3 subunit of integrin $\alpha_v\beta_3$ promotes anchorage-independent cell survival¹⁰. Further, integrin $\alpha_v\beta_3$ promotes the epithelial-mesenchymal transition of tumour cells by direct interaction with the TGF- β receptor II and binding of TGF- β . Exposure to TGF- β also leads to increased integrin $\alpha_v\beta_3$ expression^{11,12}. Expression of $\alpha_v\beta_3$ integrin has been demonstrated in several tumour entities such as melanoma and glioblastoma, as well as breast, pancreatic and prostate cancer^{7,13–16}. In melanoma, transition from benign radial growth to malignant vertical growth correlates with *de novo* expression of $\alpha_v\beta_3$ integrin¹⁷. In addition to tumour cells, integrin $\alpha_v\beta_3$ is also expressed on cells that are essential components of the tumour environment including cancer-associated fibroblasts (CAFs), tumour-associated macrophages and angiogenic endothelial cells^{18–20}.

There have been prior attempts of exploiting $\alpha_v\beta_3$ integrin as a therapeutic target. This includes immunotherapy with monoclonal antibodies (mABs) that inhibit ligand binding to $\alpha_v\beta_3$ integrin, which has been reported to be safe but only of limited efficacy²¹. Here, we report on the development of $\alpha_v\beta_3$ -specific chimeric antigen receptor (CAR) T-cells and their antitumour function in preclinical models. CARs are synthetic receptors that most commonly employ the variable heavy (VH) and variable light (VL) chains of a mAB for antigen targeting. To construct $\alpha_v\beta_3$ integrin-specific CARs, we utilized the VH and VL chains of a super-humanised mAB LM609 (hLM609), which we developed in previous work²². We have recently demonstrated that binding domain affinity and extracellular spacer domain design affect tumour cell recognition and CAR T-cell function^{23,24}, and are modulating both variables to derive an $\alpha_v\beta_3$ -CAR with optimal antitumour reactivity.

Through these iterations, we have obtained an $\alpha_v\beta_3$ -CAR that confers potent reactivity against $\alpha_v\beta_3$ -expressing hematologic and non-hematologic tumour cells *in vitro* and eliminates metastatic melanoma in a murine xenograft model *in vivo*.

Materials & Methods

Construction of $\alpha_v\beta_3$ -CAR encoding lentiviral vectors

Two codon optimised single-chain variable fragments (scFvs) were synthesized (GeneArt, ThermoFisher Scientific, Regensburg, Germany) based on mABs hLM609v7 and hLM609v11²² with a (G₄S)₃ linker to fuse VH and VL. The scFvs were cloned into ePHIV7 lentiviral vectors to generate constructs with either a long (IgG4-Fc Hinge-CH2-CH3, 229 amino acids) or short (IgG4-Fc Hinge only, 12 amino acids) extracellular spacer domain, linked to CD28 transmembrane domain, and the cytoplasmic signalling domains of CD28 and CD3 ζ ²⁴. A truncated epidermal growth factor receptor (EGFRt) was expressed *in cis* with the CAR transgene, separated by a T2A element²⁵.

Generation of $\alpha_v\beta_3$ -CAR T-cell lines

CD8⁺ and CD4⁺ T-cells were isolated by magnetic cell separation (Miltenyi, Bergisch Gladbach, Germany) from PBMCs of healthy donors and activated with anti-CD3/CD28 microbeads (ThermoFisher). T-cells were lentivirally transduced one day after activation as described previously²³. The anti-CD3/CD28 microbeads were removed 4 to 7 days after activation. At 10 to 14 days after activation, EGFRt⁺ cells were enriched by magnetic cell separation using the in-house biotinylated (ThermoFisher) mAB Cetuximab (Bristol-Myers Squibb, New York, NY, USA) and anti-biotin microbeads (Miltenyi) and expanded using a rapid expansion protocol²⁶.

In vivo experiments in xenograft mouse model

Six- to 8-week old female NOD.Cg-Prkdc^{scid} Il2rg^{tm1Wjl}/SzJ (NSG) mice were obtained from Charles River (Sulzfeld, Germany). On day 0, 1×10^6 A-375/ffluc_GFP cells were injected into the tail vein. On day 7, engraftment of the tumour cells was verified by bioluminescence imaging (BLI). Mice were then randomly assigned to treatment cohorts. Groups of mice (n = 3–6) were treated with 2.5×10^6 CD8⁺ and 2.5×10^6 CD4⁺ T-cells, either unmodified or expressing the hLM609v7/short or hLM609v11/short $\alpha_v\beta_3$ -CAR, by tail vein injection or remained untreated (n = 2). For weekly bioluminescence imaging, (IVIS Lumina, PerkinElmer, Waltham, MA, USA) the mice received 0.3 mg/g body weight D-luciferin i.p. (Biosynth, Staad, Switzerland). Living Image Software (PerkinElmer) was used for data analysis. The experimental endpoint was reached, when mice presented with either >20% weight loss or when radiance obtained by BLI exceeded 3×10^7 p/s/cm²/sr. Cytokine concentrations in mouse serum were measured using the MAGPIX System (ThermoFisher) and a Human Cytokine Magnetic 10-Plex kit (ThermoFisher). All mouse experiments were approved by the Institutional Animal Care and Use Committee of the University of Würzburg.

Results

$\alpha_v\beta_3$ integrin is expressed on hematologic and non-hematologic tumour cell lines

We analysed expression of $\alpha_v\beta_3$ integrin by flow cytometry on a panel of hematologic and non-hematologic tumour cell lines using a mAb directed against the $\alpha_v\beta_3$ integrin complex. We detected high-level $\alpha_v\beta_3$ integrin surface expression on the melanoma cell lines A-375, M14, Malme-3M, UACC-62 and UACC-257, and the triple-negative breast cancer cell line MDA-MB-231 (xMFI = MFI mAb / MFI isotype: 7.3 – 19.5); and intermediate-level expression on the T-cell acute lymphoblastic leukaemia cell line Jurkat (xMFI: 3.6) (Fig 1A). The chronic myelogenous leukaemia cell line K562 and the mantle cell lymphoma cell line JeKo-1, as well as the lung carcinoma cell line A-549 and the melanoma cell line LOX-IMVI showed only a minor increase in MFI compared to isotype control (xMFI: <2). To determine if this was due to low-level expression of $\alpha_v\beta_3$ integrin complex or rather unspecific binding, we analysed expression of the α_v and β_3 subunits on these cell lines individually (Fig 1B+S1). We detected high-level expression of α_v on LOX-IMVI, A-549 and K562, but not on the surface of JeKo-1 cells. The β_3 subunit was not expressed on LOX-IMVI and A-549 cells and only detectable at extremely low levels on K562 and JeKo-1 cells. For comparison, on K562 cells that we transduced with a lentiviral vector encoding the β_3 integrin subunit (K562_ β_3), we detected uniform, high-level expression of $\alpha_v\beta_3$ (xMFI: 13.3) (Fig 1A).

We also analysed normal T-cells, B-cells and monocytes from peripheral blood, and mobilized hematopoietic stem cells (HSCs) and did not detect relevant expression of $\alpha_v\beta_3$ integrin complex (xMFI: <2) (Fig S2+S3A). Taken together, these data affirm the prior notion, that integrin $\alpha_v\beta_3$ is expressed on malignant cells in hematologic and non-hematologic cancers, including prevalent high-level expression in melanoma cell lines. We selected the K562 and A-549 (negative); A-375, UACC-62, UACC-257 and MDA-MB-231 (positive) and K562_ β_3 cell lines (positive control) as target cells to analyse the specificity and antitumor potency of T-cells that we gene-engineered to express an $\alpha_v\beta_3$ -specific CAR.

Expression of $\alpha_v\beta_3$ -CARs in human T-cells

We designed a set of four $\alpha_v\beta_3$ -CAR constructs comprising: i. a scFv targeting domain derived from a super-humanised variant of anti- $\alpha_v\beta_3$ integrin-specific mAb LM609 with either high (hLM609v7; K_d = 3 nM) or low (hLM609v11; K_d = 160 nM) monovalent affinity²²; ii. an IgG4-Fc derived spacer of either Hinge only (short spacer, 12 amino acids) or of Hinge-CH2-CH3 (long spacer, 229 amino acids)²³. Each of the constructs contained a CD28_CD3 ζ signalling domain and was co-expressed with a truncated epidermal growth factor receptor (EGFRt) as transduction marker (Fig 2A)²⁵. We transduced each of the constructs into CD8⁺ and CD4⁺ T-cells and enriched CAR⁺ T-cells using the EGFRt marker (Fig 2B). At the end of the manufacturing process and prior to functional testing, each of the CD8⁺ and CD4⁺ $\alpha_v\beta_3$ -CAR T-cell lines was negative for $\alpha_v\beta_3$ integrin-expression by flow cytometry (Fig 2C).

$\alpha_v\beta_3$ -CAR T-cells elicit potent antitumour functions *in vitro*

We sought to determine the antitumour function of T-cells expressing our $\alpha_v\beta_3$ -CAR constructs. First, we analysed the cytolytic activity of CD8⁺ $\alpha_v\beta_3$ -CAR T-cells and found that each of the four CAR constructs conferred specific recognition and elimination of A-375, UACC-62, UACC-257, MDA-MB-231 and K562_β₃ target cells (Fig 3A). Overall, the four $\alpha_v\beta_3$ -CAR constructs with high vs. low affinity and short vs. long spacer were similarly potent and not significantly different in their ability to induce cytolysis of target cells. K562_β₃ cells were more susceptible to cytolysis compared to the melanoma cell lines and MDA-MB-231, especially at low effector-to-target cell ratios. We detected low-level recognition of native K562 cells, potentially due to very low-level expression of $\alpha_v\beta_3$ integrin complex, as suggested in our expression analysis. Accordingly, we did not detect cytolysis of A-549 cells (Fig. 3A). We also evaluated recognition of normal HSCs, and consistent with their $\alpha_v\beta_3$ -negative phenotype, viability was not affected by co-culture with $\alpha_v\beta_3$ -CAR T-cells (Fig S3B).

We confirmed that CD8⁺ and CD4⁺ $\alpha_v\beta_3$ -CAR T-cells produced IFN- γ and IL-2 after stimulation with $\alpha_v\beta_3$ -positive tumour cells (Fig 3B+C). The $\alpha_v\beta_3$ -CAR with high affinity and short spacer domain (hLM609v7/short) induced the strongest IFN- γ production, particularly in CD4⁺ T-cells (Fig. 3C). The $\alpha_v\beta_3$ -CARs with short spacer domain induced more IL-2 production compared to the constructs with long spacer. In CD4⁺ T-cells, the hLM609v7/short $\alpha_v\beta_3$ -CAR induced the strongest production of IL-2 (Fig 3B+C). Overall, we observed stronger cytokine production by CD4⁺ compared to CD8⁺ CAR T-cells. We also evaluated the proliferation of $\alpha_v\beta_3$ -CAR T-cells after stimulation with $\alpha_v\beta_3$ -positive tumour cells (Fig 3D+E). Again, there was stronger proliferation of CD4⁺ compared to CD8⁺ CAR T-cells, and the hLM609v7/short $\alpha_v\beta_3$ -CAR was superior in inducing proliferation compared to the other receptor designs. Notably, there was some background proliferation of T-cells equipped with the hLM609v7/long $\alpha_v\beta_3$ -CAR, potentially due to tonic signalling.

In summary, the data show that $\alpha_v\beta_3$ -CAR T-cells confer specific and potent antitumour functions against $\alpha_v\beta_3$ -expressing target cells *in vitro*. The data also show that the $\alpha_v\beta_3$ -CAR construct with higher affinity and short spacer domain conferred the strongest effector functions, particularly cytokine secretion and proliferation, in line with our prior observation that these parameters affects the antitumour function of CAR T-cells²³. Based on our analysis, we selected the $\alpha_v\beta_3$ -CAR constructs with short spacer domain for evaluation in an *in vivo* model.

$\alpha_v\beta_3$ -CAR T-cells are effective against metastatic melanoma *in vivo*

We established xenografts of metastatic melanoma in immunodeficient NSG mice using the aggressive A-375 cell line. We injected NSG mice with 1×10^6 firefly luciferase-labelled A-375 cells i.v. on day 0 and treated them with a single dose of 5×10^6 T-cells i.v. after 7 days (CD8:CD4 ratio = 1:1). Mice were either treated with $\alpha_v\beta_3$ -CAR T-cells (hLM609v7/short) or untransduced control T-cells derived from the same donor. We performed serial bioluminescence imaging and observed rapid tumour regression in all mice treated with $\alpha_v\beta_3$ -CAR T-cells (n=3) and rapid tumour progression in all control mice (n=3) (Fig 4A+B).

All CAR T-cell treated mice were alive until the end of the observation period on day 65 (Fig. 4C); only one mouse had a slowly progressing, singular tumour lesion in the lower back (Fig 4A+B).

In the next set of experiments, we included a group of NSG/A-375 mice that received T-cells expressing the hLM609v11/short $\alpha_v\beta_3$ -CAR to compare the higher and lower affinity $\alpha_v\beta_3$ -CAR constructs. On day 3 and day 7 after adoptive T-cell transfer, we analysed peripheral blood samples and confirmed T-cell engraftment in all treatment-groups (Fig 5A). Between day 3 and day 7, the percentage of $\alpha_v\beta_3$ -CAR T-cells increased, in particular in the group of mice that had received the lower affinity hLM609v11/short $\alpha_v\beta_3$ -CAR. In serum samples, we measured elevated concentrations of IFN- γ and GM-CSF in mice that received $\alpha_v\beta_3$ -CAR T-cells, but not in mice that had received control T-cells (Fig 5B). Interestingly, also the cytokine concentrations were higher in mice that had been treated with the lower affinity hLM609v11/short compared to the higher affinity hLM609v7/short $\alpha_v\beta_3$ -CAR. Treatment with $\alpha_v\beta_3$ -CAR T-cells conferred a potent antitumour effect. On day 3 after T-cell transfer (day 10 after tumour inoculation), we already detected lower levels of bioluminescence signal in all of the mice that had received CAR T-cells, whereas there was increasing bioluminescence signal in all mice in the control groups that had either received untransduced T-cells or no treatment (Fig 5C). By day 28, the bioluminescence signal had reached background levels in 4 out of 6 mice in the hLM609v7/short, and 5 out of 6 mice in the hLM609v11/short $\alpha_v\beta_3$ -CAR T-cell groups, respectively, indicating that all tumour lesions had been eradicated (Fig 5C+D). Out of the 12 mice treated with $\alpha_v\beta_3$ -CAR T-cells 3 did not reach the background bioluminescence signal and had a recurrent tumour at the same site as one of the first lesions. Three of the 6 mice in the hLM609v7/short treatment group were lost to follow-up for reasons unrelated to tumour progression. Kaplan-Meier analysis showed that by day 44, all of the mice in the control groups had to be sacrificed due to tumour progression (Fig 5E). In contrast, all of the mice that completed follow-up were alive in the hLM609v7 $\alpha_v\beta_3$ -CAR (3 out of 3), and all of the mice were alive in the hLM609v11 $\alpha_v\beta_3$ -CAR cohort (6 out of 6). Bone marrow analysis at the end of the experiment confirmed that CAR T-cells and untransduced T-cells had persisted for the entire duration of the experiment (Fig 5F).

Taken together, these data show that $\alpha_v\beta_3$ -CAR T-cells confer potent antitumour efficacy *in vivo*. Several lines of evidence, including stronger CAR T-cell expansion and cytokine secretion, and a higher rate of complete responses indicate that $\alpha_v\beta_3$ -CAR T-cells with the lower-affinity binding domain hLM609v11 conferred stronger antitumor reactivity than $\alpha_v\beta_3$ -CAR T-cells with the higher-affinity hLM609v7 binding domain *in vivo*, which reverses the hierarchy established in our *in vitro* analysis.

Conclusions

Adoptive immunotherapy with gene-engineered CAR T-cells has curative potential against advanced hematologic malignancies²⁷. At present, significant efforts are being invested to extend the clinical success that has been obtained with CD19-specific CAR T-cells in B-cell leukaemia and lymphoma, to prevalent non-hematologic tumours, which requires the identification and validation of novel target antigens. Here, we demonstrate that CAR T-cells

specific for $\alpha_v\beta_3$ integrin exhibit potent antitumor reactivity, including effective tumour cell lysis, as well as cytokine production and proliferation after stimulation with $\alpha_v\beta_3$ -expressing cancer cells *in vitro*. Further, we demonstrate that $\alpha_v\beta_3$ -CAR T-cells are capable of completely eradicating established A-375 melanoma in a xenograft model in mice.

Our data show that $\alpha_v\beta_3$ -CAR constructs with hLM609-derived binding domains confer superior antitumour function when equipped with a short IgG-Fc Hinge rather than a long IgG-Fc Hinge-CH2-CH3 spacer domain. This is consistent with our previous observation with CD19 and ROR1-specific CARs, showing that the length of the extracellular spacer domain affects tumour cell recognition and CAR T-cell function, likely because of the spatial interaction of CAR and tumour antigen, and the localisation of the targeted epitope^{23,24}. The paradigm that emerged from our previous studies is that the 'long' spacer domain is optimal for targeting epitopes that are proximal to the tumour-cell membrane, while a 'short' spacer domain is optimal for targeting membrane-distal epitopes. The mAb LM609 recognises a membrane-distal epitope of integrin $\alpha_v\beta_3$ ²⁸ and accordingly, our data that $\alpha_v\beta_3$ -CAR constructs with 'short' spacer domain confer the strongest antitumour functions, are in line with this paradigm.

We show that $\alpha_v\beta_3$ -CAR T-cells are able to eradicate metastatic A-375 melanoma in an NSG mouse xenograft model. The A-375 melanoma model is commonly used to evaluate novel anticancer agents and notably, the efficacy that we observed with $\alpha_v\beta_3$ -CAR T-cells in our study is superior to the efficacy that has recently been reported for several alternative investigational treatments, including a combination treatment of oncolytic adenovirus and dacarbazine chemotherapy, and itraconazole, that both achieved tumour reduction but not tumour clearance like in our study^{29,30}.

Interestingly, we observed stronger CAR T-cell expansion and cytokine secretion in mice that had been treated with the lower-affinity hLM609v11 $\alpha_v\beta_3$ -CAR, indicating the lower affinity receptor had induced stronger T-cell activation *in vivo*. In contrast, in our *in vitro* analysis, the higher-affinity hLM609v7 $\alpha_v\beta_3$ -CAR had induced stronger cytokine secretion and proliferation. Other investigators have reported similar findings with CAR T-cells targeting ErbB2³¹. A potential explanation is that the lower-affinity hLM609v11 binding domain has a three-times faster off-rate than the higher-affinity variant hLM609v7 ($16 \times 10^{-4} \text{ s}^{-1}$ versus $5.4 \times 10^{-4} \text{ s}^{-1}$ measured for the corresponding monovalent Fab) and therefore, hLM609v11 CAR T-cells are more likely to sequentially interact with tumour cells and thus, may receive a higher net activation signal. Experiments with additional affinity variants of hLM609 are warranted in order to define the 'sweet spot' of hLM609 affinity that permits maximum antitumour function of the $\alpha_v\beta_3$ -CAR.

In this study, we used super-humanised LM609 VH and VL variants to derive $\alpha_v\beta_3$ -CAR targeting domains with minimal immunogenicity. Indeed, we and others have demonstrated in previous work that immune responses directed against immunogenic epitopes located in murine VH/VL CAR targeting domain can lead to rejection of CAR T-cells, which may limit or abrogate the antitumour effect^{32,33}. Notably, the super-humanised hLM609v7 and hLM609v11 variants employed in our $\alpha_v\beta_3$ -CARs retained only the third complementarity

determining region (CDR) of the parental mouse mAB LM609 VH and VL chains. All other CDRs and framework regions were replaced by human amino acid sequences²².

A previous study has reported on the construction of an $\alpha_v\beta_3$ -CAR that instead of a mAB-derived scFv, utilized a modified echistatin peptide, a disintegrin, as targeting moiety, which binds to both human and mouse $\alpha_v\beta_3$ integrin³⁴. These $\alpha_v\beta_3$ -specific CAR T-cells were tested in a syngeneic mouse model against B16 melanoma and inhibited tumour growth, but did not achieve tumour eradication. Further, this study showed that echistatin-based $\alpha_v\beta_3$ -CAR T-cells damage tumour vasculature, due to $\alpha_v\beta_3$ -expression on tumour endothelium, which was evident from haematomas in the tumour tissue. Encouragingly, the adoptive transfer of echistatin-based $\alpha_v\beta_3$ -CAR T-cells did not cause any evident toxicity to normal tissues³⁴. Expression of $\alpha_v\beta_3$ integrin has been reported on several healthy tissues including angiogenic endothelial cells, osteoclasts, vascular smooth muscle cells, platelets, macrophages and HSCs^{4,35–37}. The expression density and conformation of $\alpha_v\beta_3$ may be modulated, e.g. under inflammatory conditions^{1–3}.

Notably, clinical studies with the two humanised LM609 mABs vitaxin and abegrin did not report any severe adverse events, and did not report toxicity to these normal tissues and cell subsets^{38–41}. While encouraging for the clinical translation of adoptive therapy with $\alpha_v\beta_3$ -CAR T-cells, the safety data obtained with mABs have to be considered with caution because of the substantially higher potency of CAR-T-cells. In a first-in-human study with $\alpha_v\beta_3$ -CAR T-cells, the lower-affinity hLM609v11 scFv may be a preferable targeting domain because of data obtained with other CAR constructs indicating that higher affinity may come at the expense of reduced selectivity, and that higher affinity scFvs are more likely to confer recognition of normal tissues that express the targeted antigen with low density^{31,42,43}. In a clinical study, it is advisable to equip CAR T-cells with a depletion marker or suicide gene to provide a safety switch in case of toxicity⁴⁴. The $\alpha_v\beta_3$ -CAR T-cells presented in our study are equipped with an EGFRt marker that we have shown can be used to deplete CAR T-cells by administering the anti-EGFR mAB cetuximab²⁵.

Our data suggest that adoptive therapy with $\alpha_v\beta_3$ -CAR T-cells has the potential to confer greater therapeutic efficacy compared to immunotherapy with anti- $\alpha_v\beta_3$ mABs. The anti- $\alpha_v\beta_3$ mABs that were employed in previous clinical studies exerted their mechanism of action by sterically hindering the binding of RGD-ligands to $\alpha_v\beta_3$ integrin to inhibit tumour vascularisation²⁸. We demonstrate that $\alpha_v\beta_3$ -CAR T-cells exert a distinct set of effector mechanisms including direct cytolytic activity against $\alpha_v\beta_3$ -positive tumour cells. In addition, we anticipate that $\alpha_v\beta_3$ -CAR T-cells will also alter the tumour microenvironment and limit tumour angiogenesis by destruction of $\alpha_v\beta_3$ -expressing cancer associated fibroblasts and endothelial cells in tumour-associated blood vessels. Further, the expression of $\alpha_v\beta_3$ on tumour vasculature should facilitate the migration of $\alpha_v\beta_3$ -CAR T-cells to and invasion into primary and metastatic tumour lesions. Indeed, in prior work, other investigators have equipped primary lymphocytes with a membrane-bound fusion-molecule that targets integrin $\alpha_v\beta_3$ through the disintegrin kistrin and observed increased lymphocyte infiltration of tumour sites⁴⁵.

A recent observation is the strong resistance of $\alpha_v\beta_3$ -expressing cancer cells to cisplatin and doxorubicin, the standard-of-care chemotherapy agents for several solid tumour malignancies⁴⁶. This observation suggests, that adoptive immunotherapy with $\alpha_v\beta_3$ -CAR T-cells may be used either concomitantly or sequentially to chemotherapy in order to delete chemotherapy-resistant tumour cells and improve therapeutic outcomes.

Collectively, our data introduce $\alpha_v\beta_3$ integrin as a novel target for CAR T-cells with potential utility in several prevalent solid tumours. Our data affirm our previous notion that binding domain affinity and spacer length can be calibrated to augment the antitumour reactivity of CARs. Because $\alpha_v\beta_3$ integrin is expressed on primary and metastatic tumour cells, endothelial cells of tumour vasculature and tumour stroma, $\alpha_v\beta_3$ -CAR T-cells bear significant therapeutic potential in a clinical setting.

Supplementary Material

Refer to Web version on PubMed Central for supplementary material.

Acknowledgements

M.H. was supported by the Young Scholar Program of the Bavarian Academy of Sciences (Junges Kolleg, Bayerische Akademie der Wissenschaften), and is an extraordinary member of the Bavarian Academy of Sciences. This work was supported by grants from the German Cancer Aid (Deutsche Krebshilfe e.V., Max Eder Program 110313 to M.H.), the IZKF Würzburg (Interdisziplinäres Zentrum für Klinische Forschung, Universitätsklinikum Würzburg, Projekt Z-4/109, D-244, B-354 to M.H.), and NIH grant R01 CA 181258 (to C.R.). The authors thank Professor Bastian Schilling (Universitätsklinikum Würzburg) for providing the Malme-3M, M14, UACC-62, UACC-257, and LOX-IMVI cell lines, and Professor Halvard Bönig (Goethe-Universität Frankfurt am Main) for providing normal hematopoietic stem cells.

Appendix

Supplemental Materials & Methods

Human subjects

Peripheral blood was obtained from healthy donors after written informed consent to participate in research protocols approved by the Institutional Review Board of the University of Würzburg. Normal hematopoietic stem cells were obtained from healthy donors after written informed consent to participate in research protocols approved by the Institutional Review Board of the University of Frankfurt and kindly provided by Professor Halvard Bönig (University of Frankfurt/Blutspendedienst DRK, Frankfurt, Germany)

Cell lines

The K562 (ACC 10), JeKo-1 (ACC 553), Jurkat (ACC 282), A-549 (ACC 107) and MDA-MB-231 cell lines (ACC 732) were obtained from the Leibniz Institute DSMZ-German Collection of Microorganisms and Cell Cultures (Braunschweig, Germany) and cultured in RPMI-1640 supplemented with 10% fetal bovine serum, 2 mM glutamine and 100 U/ml penicillin/streptomycin. A-375 (CRL-1619) were obtained from ATCC (Manassas, VA, USA) and cultured in DMEM supplemented with 10% fetal bovine serum, 2 mM glutamine and 100 U/ml penicillin/streptomycin. The Malme-3M (RRID:CVCL_1438), M14 (RRID:CVCL_1395), UACC-62 (RRID:CVCL_1780), UACC-257 (RRID:CVCL_1779)

and LOX-IMVI (RRID:CVCL_1381) were a kind gift of Professor Bastian Schilling (Universitätsklinikum Würzburg, Germany) and cultured in RPMI-1640 supplemented with 10% fetal bovine serum, 2 mM glutamine and 100 U/ml penicillin/streptomycin. K562 cells expressing full-length human β_3 integrin (K562_ β_3) were generated by lentiviral transduction. K562, K562_ β_3 , JeKo-1, MDA-MB-231, A-549, UACC-62, UACC-257 and A-375 were transduced with a lentiviral vector encoding firefly luciferase (ffluc) and green fluorescent protein (GFP) transgenes.

Flow Cytometry

All flow cytometric analyses were done on a BD FACSCanto II (BD Biosciences, Heidelberg, Germany) and analysed with FlowJo V10.2 software (FlowJo, Ashland, OR, USA). Fluorochrome-labelled mABs against CD4 and CD8 were purchased from Miltenyi Biotec (Bergisch-Gladbach, Germany) or BD. mABs against CD3, CD14, CD19, CD34, CD45, CD51 (α_v), CD51/CD61 ($\alpha_v\beta_3$, clone 23C6), CD61 (β_3) and corresponding isotype controls were purchased from BioLegend (San Diego, CA, USA). All mABs were used according to the manufacturer's instructions. The anti-EGFR mAB Cetuximab (Bristol-Myers Squibb, New York, NY, USA) was labelled in-house with Alexa-647 following the manufacturer's instructions (ThermoFisher).

Analysis of CAR T-cell function *in vitro*

The lysis of ffluc_GFP transduced target cells was determined in a bioluminescence-based assay^{1,2} with 5×10^3 target cells and CD8⁺ T-cells at the indicated effector:target cell ratios. Luciferin substrate was added at the beginning of the experiment and, after 4 h of incubation, the luminescence signal was measured with an Infinite 200 PRO plate reader (Tecan, Männedorf, Switzerland). Specific lysis conferred by CAR T-cells was calculated using the standard formula, using untransduced T-cells as reference. ELISAs (BioLegend) were used to quantify the IFN- γ and IL-2 concentrations in supernatants obtained after a 22-hour co-culture of T-cells with target cells (effector:target cell ratio = 5:1) with 1×10^5 T-cells in 200 μ l medium. For analysis of proliferation, T-cells were labelled with 0.1 μ M carboxyfluorescein succinimidyl ester (CFSE, ThermoFisher), and 5×10^4 labelled T-cells co-cultured with irradiated tumour cells (effector:target cell ratio = 5:1) in 200 μ l medium. After 72 h, T-cells were labelled with mABs against CD4 and CD8. Samples were measured by flow cytometry and division of T-cells was assessed by CFSE dilution. For calculation of the proliferation index, the proliferation of T-cells in basal medium was subtracted from corresponding samples. The proliferation index was calculated using the standard formula in FlowJo software. The lysis of CD34⁺ hematopoietic stem cells (HSCs) was assessed in a flow cytometry-based assay. 5×10^3 HSCs and T-cells were co-cultured at the indicated effector:target cell ratios. After 4 h and 24 h, samples were stained with mABs against CD34 and CD3 to discriminate T-cells and HSCs, and 7-AAD to discriminate live and dead cells. 123count eBeads (ThermoFisher) were used according to the manufacturer's instructions to determine the number of live HSCs. The proportion of living HSCs in relation to medium control was calculated using the standard formula.

Statistical analysis

Statistical analyses were performed with GraphPad Prism 6.07 software (GraphPad Software, San Diego, CA, USA). For *in vitro* cytokine and proliferation assays, the statistical significance of $n = 3$ experiments with T-cells from $n = 3$ healthy donors was evaluated by two-way ANOVA with Tukey's multiple comparison test. *In vivo* cytokine secretion was evaluated by Kruskal-Wallis test with Dunn's multiple comparison test, and survival was evaluated by Mantel-Cox test with Bonferroni corrected threshold. Results with $p < 0.05$ were considered significant.

References

1. Hynes RO. Integrins: bidirectional, allosteric signaling machines. *Cell*. 2002;110(6):673–687. doi:10.1016/S0092-8674(02)00971-6. [PubMed: 12297042]
2. Campbell ID, Humphries MJ. Integrin structure, activation, and interactions. *Cold Spring Harb Perspect Biol* 2011;3(3):a004994–a004994. doi:10.1101/cshperspect.a004994. [PubMed: 21421922]
3. Desgrosellier JS, Cheresh DA. Integrins in cancer: biological implications and therapeutic opportunities. *Nat Rev Cancer*. 2010;10(1):9–22. doi:10.1038/nrc2748. [PubMed: 20029421]
4. Felding-Habermann B, Cheresh DA. Vitronectin and its receptors. *Curr Opin Cell Biol*. 1993;5(5):864–868. doi:10.1016/0955-0674(93)90036-P. [PubMed: 7694604]
5. Petitsclerc E, Strömblad S, von Schalscha TL, et al. Integrin alpha(v)beta3 promotes M21 melanoma growth in human skin by regulating tumor cell survival. *Cancer Res*. 1999;59(11):2724–2730. <http://www.ncbi.nlm.nih.gov/pubmed/10363998>. Accessed January 19, 2018. [PubMed: 10363998]
6. Liapis H, Flath A, Kitazawa S. Integrin $\alpha v \beta 3$ Expression by Bone-residing Breast Cancer Metastases. *Diagnostic Mol Pathol*. 1996;5(2):127–135. doi:10.1097/00019606-199606000-00008.
7. Sloan EK, Pouliot N, Stanley KL, et al. Tumor-specific expression of $\alpha v \beta 3$ integrin promotes spontaneous metastasis of breast cancer to bone. *Breast Cancer Res*. 2006;8(2):R20. doi:10.1186/bcr1398. [PubMed: 16608535]
8. Felding-Habermann B, O'Toole TE, Smith JW, et al. Integrin activation controls metastasis in human breast cancer. *Proc Natl Acad Sci U S A*. 2001;98(4):1853–1858. doi:10.1073/pnas.98.4.1853. [PubMed: 11172040]
9. Gay LJ, Felding-Habermann B. Contribution of platelets to tumour metastasis. *Nat Rev Cancer*. 2011;11(2):123–134. doi:10.1038/nrc3004. [PubMed: 21258396]
10. Desgrosellier JS, Barnes LA, Shields DJ, et al. An integrin alpha(v)beta(3)-c-Src oncogenic unit promotes anchorage-independence and tumor progression. *Nat Med*. 2009;15(10):1163–1169. doi:10.1038/nm.2009. [PubMed: 19734908]
11. Ludbrook SB, Barry ST, Delves CJ, Horgan CMT. The integrin $\alpha v \beta 3$ is a receptor for the latency-associated peptides of transforming growth factors beta1 and beta3. *Biochem J*. 2003;369(Pt 2):311–318. doi:10.1042/BJ20020809. [PubMed: 12358597]
12. Galliher AJ, Schiemann WP. Beta3 integrin and Src facilitate transforming growth factor-beta mediated induction of epithelial-mesenchymal transition in mammary epithelial cells. *Breast Cancer Res*. 2006;8(4):R42. doi:10.1186/bcr1524. [PubMed: 16859511]
13. Albelda SM, Mette SA, Elder DE, et al. Integrin distribution in malignant melanoma: association of the beta 3 subunit with tumor progression. *Cancer Res*. 1990;50(20):6757–6764. <http://www.ncbi.nlm.nih.gov/pubmed/2208139>. Accessed December 13, 2017. [PubMed: 2208139]
14. Hosotani R, Kawaguchi M, Masui T, et al. Expression of integrin $\alpha v \beta 3$ in pancreatic carcinoma: relation to MMP-2 activation and lymph node metastasis. *Pancreas*. 2002;25(2):e30–5. doi:00006676-200208000-00021 [pii]. [PubMed: 12142752]
15. McCabe NP, De S, Vasanji A, Brainard J, Byzova T V. Prostate cancer specific integrin $\alpha v \beta 3$ modulates bone metastatic growth and tissue remodeling. *Oncogene*. 2007;26(42):6238–6243. doi:10.1038/sj.onc.1210429. [PubMed: 17369840]

16. Schnell O, Krebs B, Wagner E, et al. Expression of integrin $\alpha v\beta 3$ in gliomas correlates with tumor grade and is not restricted to tumor vasculature. *Brain Pathol.* 2008;18(3):378–386. doi:10.1111/j.1750-3639.2008.00137.x. [PubMed: 18394009]
17. Hsu MY, Shih DT, Meier FE, et al. Adenoviral gene transfer of beta3 integrin subunit induces conversion from radial to vertical growth phase in primary human melanoma. *Am J Pathol.* 1998;153(5):1435–1442. doi:10.1016/S0002-9440(10)65730-6. [PubMed: 9811334]
18. Brooks PC, Montgomery AM, Rosenfeld M, et al. Integrin alpha v beta 3 antagonists promote tumor regression by inducing apoptosis of angiogenic blood vessels. *Cell.* 1994;79(7):1157–1164. <http://www.ncbi.nlm.nih.gov/pubmed/7528107>. [PubMed: 7528107]
19. Zhou W, Ke SQ, Huang Z, et al. Periostin secreted by glioblastoma stem cells recruits M2 tumour-associated macrophages and promotes malignant growth. *Nat Cell Biol.* 2015;17(2):170–182. doi:10.1038/ncb3090. [PubMed: 25580734]
20. Attieh Y, Clark AG, Grass C, et al. Cancer-associated fibroblasts lead tumor invasion through integrin- $\beta 3$ -dependent fibronectin assembly. *J Cell Biol.* 2017;216(11):3509–3520. doi:10.1083/jcb.201702033. [PubMed: 28931556]
21. Raab-Westphal S, Marshall JF, Goodman SL. Integrins as therapeutic targets: Successes and cancers. *Cancers (Basel).* 2017;9(9):1–28. doi:10.3390/cancers9090110.
22. Rader C, Cheresch DA, Barbas CF, 3rd. A phage display approach for rapid antibody humanization: designed combinatorial V gene libraries. *Proc Natl Acad Sci U S A.* 1998;95(15):8910–8915. doi:10.1073/pnas.95.15.8910. [PubMed: 9671778]
23. Hudecek M, Lupo-Stanghellini M-T, Kosasih PL, et al. Receptor Affinity and Extracellular Domain Modifications Affect Tumor Recognition by ROR1-Specific Chimeric Antigen Receptor T Cells. *Clin Cancer Res.* 2013;19(12):3153–3164. doi:10.1158/1078-0432.CCR-13-0330. [PubMed: 23620405]
24. Hudecek M, Sommermeyer D, Kosasih PL, et al. The Nonsignaling Extracellular Spacer Domain of Chimeric Antigen Receptors Is Decisive for In Vivo Antitumor Activity. *Cancer Immunol Res.* 2015;3(2):125–135. doi:10.1158/2326-6066.CIR-14-0127. [PubMed: 25212991]
25. Wang X, Chang W-C, Wong CW, et al. A transgene-encoded cell surface polypeptide for selection, in vivo tracking, and ablation of engineered cells. *Blood.* 2011;118(5):1255–1263. doi:10.1182/blood-2011-02-337360. [PubMed: 21653320]
26. Riddell SR, Greenberg PD. The use of anti-CD3 and anti-CD28 monoclonal antibodies to clone and expand human antigen-specific T cells. *J Immunol Methods.* 1990;128(2):189–201. <http://www.ncbi.nlm.nih.gov/pubmed/1691237>. Accessed February 14, 2018. [PubMed: 1691237]
27. Turtle CJ, Riddell SR, Maloney DG. CD19-Targeted chimeric antigen receptor-modified T-cell immunotherapy for B-cell malignancies. *Clin Pharmacol Ther.* 2016;100(3):252–258. doi:10.1002/cpt.392. [PubMed: 27170467]
28. Borst AJ, James ZM, Zagotta WN, et al. The Therapeutic Antibody LM609 Selectively Inhibits Ligand Binding to Human $\alpha V\beta 3$ Integrin via Steric Hindrance. *Structure.* 2017;25(11):1732–1739.e5. doi:10.1016/j.str.2017.09.007. [PubMed: 29033288]
29. Yang C, Cao H, Liu N, Xu K, Ding M, Mao L. Oncolytic adenovirus expressing interleukin-18 improves antitumor activity of dacarbazine for malignant melanoma. *Drug Des Devel Ther.* 2016;10:3755–3761. doi:10.2147/DDDT.S115121.
30. Liang G, Liu M, Wang Q, et al. Itraconazole exerts its anti-melanoma effect by suppressing Hedgehog, Wnt, and PI3K/mTOR signaling pathways. *Oncotarget.* 2017;8(17):28510–28525. doi:10.18632/oncotarget.15324. [PubMed: 28212537]
31. Liu X, Jiang S, Fang C, et al. Affinity-tuned ErbB2 or EGFR chimeric antigen receptor T cells exhibit an increased therapeutic index against tumors in mice. *Cancer Res.* 2015;75(17):3596–3607. doi:10.1158/0008-5472.CAN-15-0159. [PubMed: 26330166]
32. Lamers CHJ, Willemsen R, van Elzakker P, et al. Immune responses to transgene and retroviral vector in patients treated with ex vivo-engineered T cells. *Blood.* 2011;117(1):72–82. doi:10.1182/blood-2010-07-294520. [PubMed: 20889925]
33. Turtle CJ, Hanafi L-A, Berger C, et al. CD19 CAR-T cells of defined CD4+:CD8+ composition in adult B cell ALL patients. *J Clin Invest.* 2016;126(6):2123–2138. doi:10.1172/JCI85309. [PubMed: 27111235]

34. Fu X, Rivera A, Tao L, Zhang X. Genetically modified T cells targeting neovasculature efficiently destroy tumor blood vessels, shrink established solid tumors and increase nanoparticle delivery. *Int J cancer*. 2013;133(10):2483–2492. doi:10.1002/ijc.28269. [PubMed: 23661285]
35. Clover J, Dodds RA, Gowen M. Integrin subunit expression by human osteoblasts and osteoclasts in situ and in culture. *J Cell Sci*. 1992;103(1):267–271. doi:10.1016/S8756-3282(96)00281-5. [PubMed: 1429908]
36. Brooks PC, Clark RA, Cheresh DA. Requirement of vascular integrin alpha v beta 3 for angiogenesis. *Science*. 1994;264(5158):569–571. [PubMed: 7512751]
37. Umemoto T, Yamato M, Ishihara J, et al. Integrin- $\alpha v \beta 3$ regulates thrombopoietin-mediated maintenance of hematopoietic stem cells. *Blood*. 2012;119(1):83–94. doi:10.1182/blood-2011-02-335430. [PubMed: 22096247]
38. Gutheil JC, Campbell TN, Pierce PR, et al. Targeted antiangiogenic therapy for cancer using Vitaxin: a humanized monoclonal antibody to the integrin $\alpha v \beta 3$. *Clin Cancer Res*. 2000;6(8):3056–3061. [PubMed: 10955784]
39. McNeel DG, Eickhoff J, Lee FT, et al. Phase I Trial of a Monoclonal Antibody Specific for $\alpha v \beta 3$ Integrin (MEDI-522) in Patients with Advanced Malignancies, Including an Assessment of Effect on Tumor Perfusion. *Clin Cancer Res*. 2005;11(21):7851 LP–7860. doi:10.1158/1078-0432.CCR-05-0262. [PubMed: 16278408]
40. Delbaldo C, Raymond E, Vera K, et al. Phase I and pharmacokinetic study of etaracizumab (Abegrin™), a humanized monoclonal antibody against $\alpha v \beta 3$ integrin receptor, in patients with advanced solid tumors. *Invest New Drugs*. 2008;26(1):35–43. doi:10.1007/s10637-007-9077-0. [PubMed: 17876527]
41. Hersey P, Sosman J, O'Day S, et al. A randomized phase 2 study of etaracizumab, a monoclonal antibody against integrin $\alpha v \beta 3$, \pm dacarbazine in patients with stage IV metastatic melanoma. *Cancer*. 2010;116(6):1526–1534. doi:10.1002/cncr.24821. [PubMed: 20108344]
42. Chmielewski M, Hombach A, Heuser C, Adams GP, Abken H. T Cell Activation by Antibody-Like Immunoreceptors: Increase in Affinity of the Single-Chain Fragment Domain above Threshold Does Not Increase T Cell Activation against Antigen-Positive Target Cells but Decreases Selectivity. *J Immunol*. 2004;173(12):7647–7653. doi:10.4049/jimmunol.173.12.7647. [PubMed: 15585893]
43. Caruso HG, Hurton L V, Najjar A, et al. Tuning sensitivity of CAR to EGFR density limits recognition of normal tissue while maintaining potent antitumor activity. *Cancer Res*. 2015;75(17):3505–3518. doi:10.1158/0008-5472.CAN-15-0139. [PubMed: 26330164]
44. Casucci M, Hawkins RE, Dotti G, Bondanza A. Overcoming the toxicity hurdles of genetically targeted T cells. *Cancer Immunol Immunother*. 2015;64(1):123–130. doi:10.1007/s00262-014-1641-9. [PubMed: 25488419]
45. Legler DF, Johnson-Léger C, Wiedle G, Bron C, Imhof BA. The $\alpha v \beta 3$ integrin as a tumor homing ligand for lymphocytes. *Eur J Immunol*. 2004;34(6):1608–1616. doi:10.1002/eji.200424938. [PubMed: 15162430]
46. Brozovic A, Majhen D, Roje V, et al. $\alpha v \beta 3$ Integrin-mediated drug resistance in human laryngeal carcinoma cells is caused by glutathione-dependent elimination of drug-induced reactive oxidative species. *Mol Pharmacol*. 2008;74(1):298–306. doi:10.1124/mol.107.043836. [PubMed: 18441044]

Supplementary References

1. Brown CE, Wright CL, Naranjo A, et al. Biophotonic cytotoxicity assay for high-throughput screening of cytolytic killing. *J Immunol Methods*. 2005;297(1–2):39–52. doi:10.1016/j.jim.2004.11.021. [PubMed: 1577929]
2. Monjezi R, Miskey C, Gogishvili T, et al. Enhanced CAR T-cell engineering using non-viral Sleeping Beauty transposition from minicircle vectors. *Leukemia*. 2017;31(1):186–194. doi:10.1038/leu.2016.180. [PubMed: 27491640]

Clinical Implications

Adoptive immunotherapy with CAR T-cells has been shown to be effective in advanced hematologic malignancies. Here, we demonstrate that $\alpha_v\beta_3$ -expressing tumours can be targeted with $\alpha_v\beta_3$ -specific CAR-T-cells. Integrin $\alpha_v\beta_3$ is expressed on several prevalent epithelial, mesenchymal and neuroectodermal cancers, including melanoma, glioblastoma, breast, pancreatic and prostate cancer. CAR T-cells exert a unique mode of action that can overcome resistance to conventional chemoradiotherapy and antibody-mediated immunotherapy. Intriguingly, $\alpha_v\beta_3$ integrin is also present on tumour vasculature and tumour stroma cells, e.g. cancer associated fibroblasts suggesting, that $\alpha_v\beta_3$ -CAR T-cells would be able to effectively migrate to and invade a solid tumour mass. Our data encourage the initiation of clinical studies to assess the safety and efficacy of $\alpha_v\beta_3$ -CAR T-cell therapy.

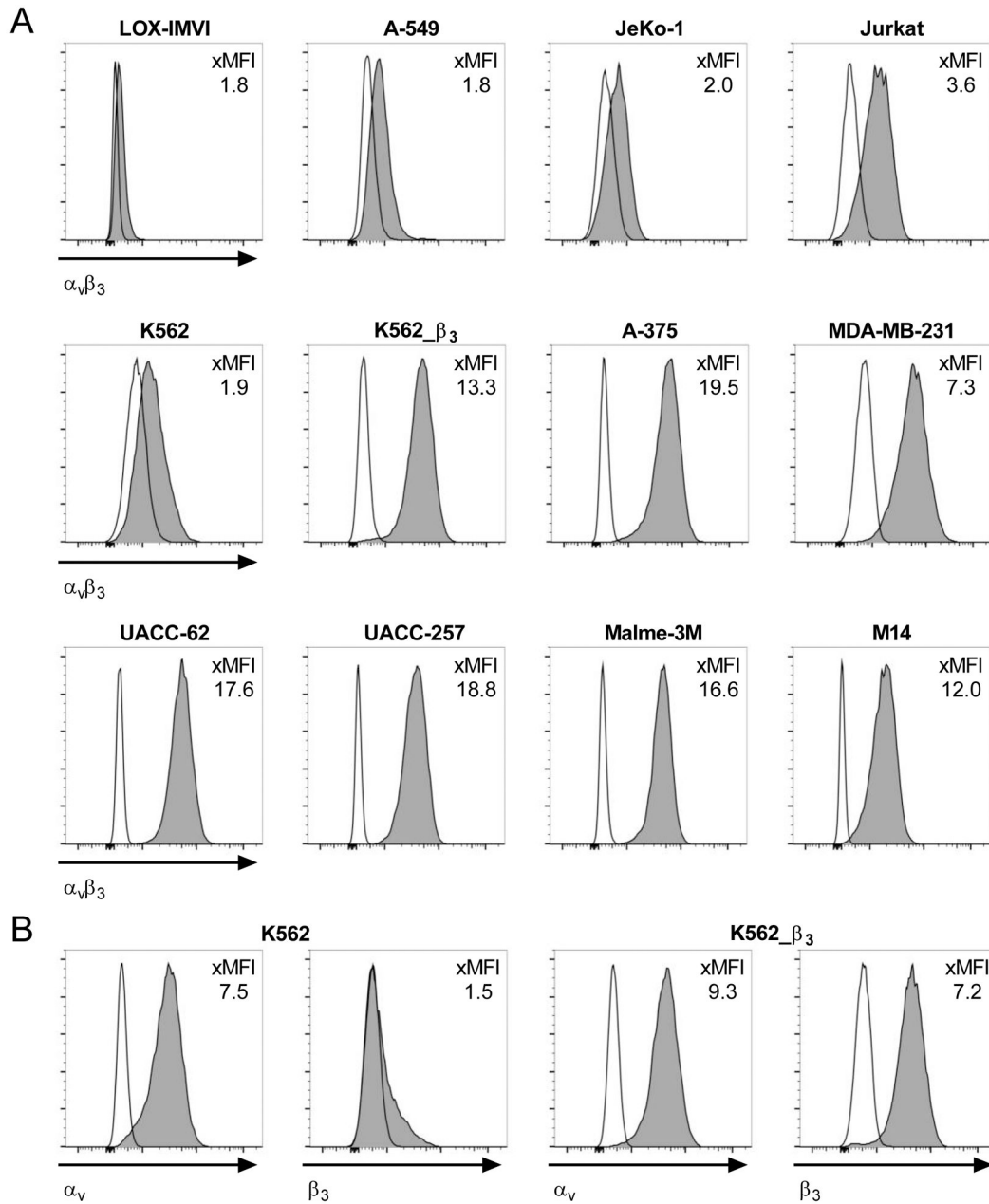


Figure 1. $\alpha_v\beta_3$ integrin is expressed on hematologic and non-hematologic tumour cell lines. (A) Flow cytometric analysis of $\alpha_v\beta_3$ -heterodimer expression and (B) α_v and β_3 integrin-subunit expression on tumour cell lines. The ratio between the geometric mean fluorescent intensity of anti- $\alpha_v\beta_3$, anti- α_v or anti- β_3 mABs (dark grey) and their corresponding isotype controls (clear) is provided as fold MFI (xMFI).

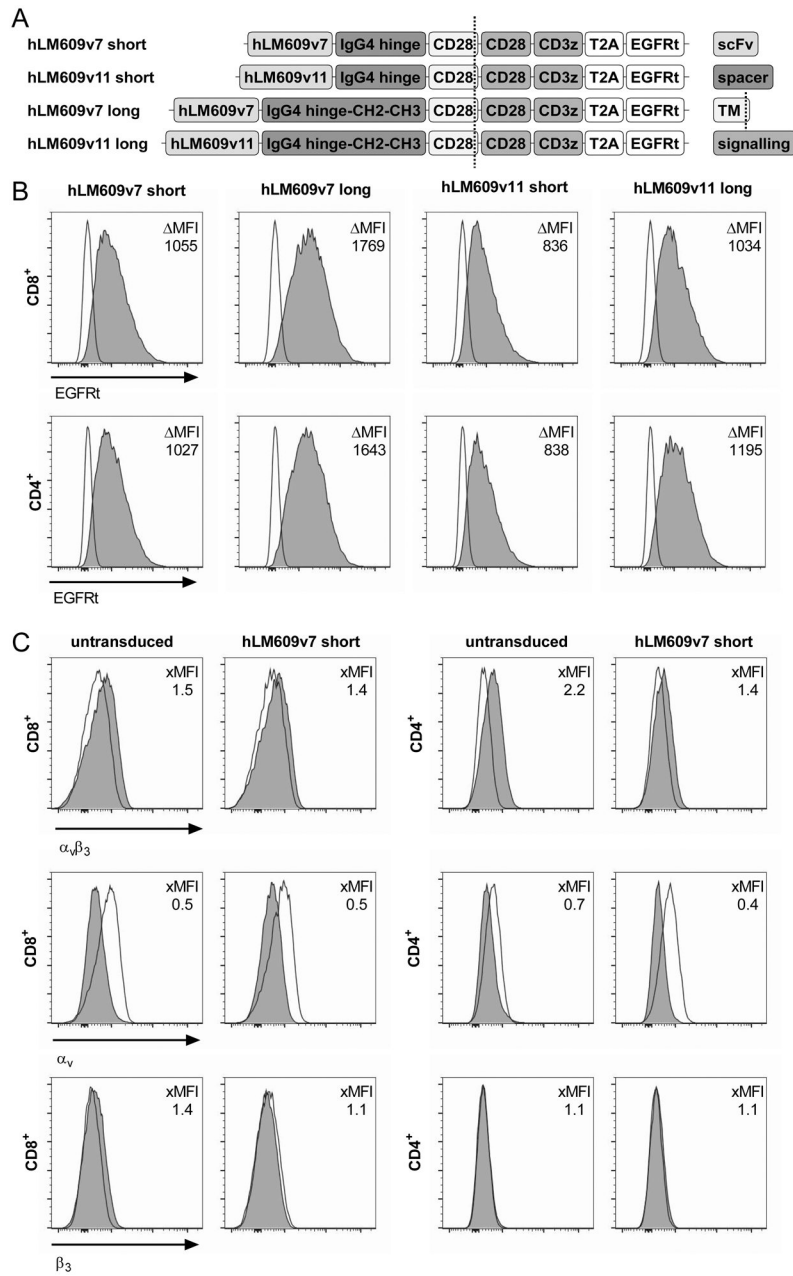


Figure 2. Design of $\alpha_v\beta_3$ -CARs and phenotype of $\alpha_v\beta_3$ -CAR T-cell lines. (A) Schematic depiction of the $\alpha_v\beta_3$ -CAR panel. (B) Flow cytometric analysis of EGFRt expression on CD8⁺ and CD4⁺ T-cells transduced with $\alpha_v\beta_3$ -CARs to assess transgene expression. The ΔMFI depicts the difference in geometric mean fluorescent intensity between CAR-transduced (dark grey) and untransduced (clear) samples. (C) Expression of $\alpha_v\beta_3$ -heterodimer and corresponding subunits on untransduced and $\alpha_v\beta_3$ -CAR-modified T-cells after expansion.

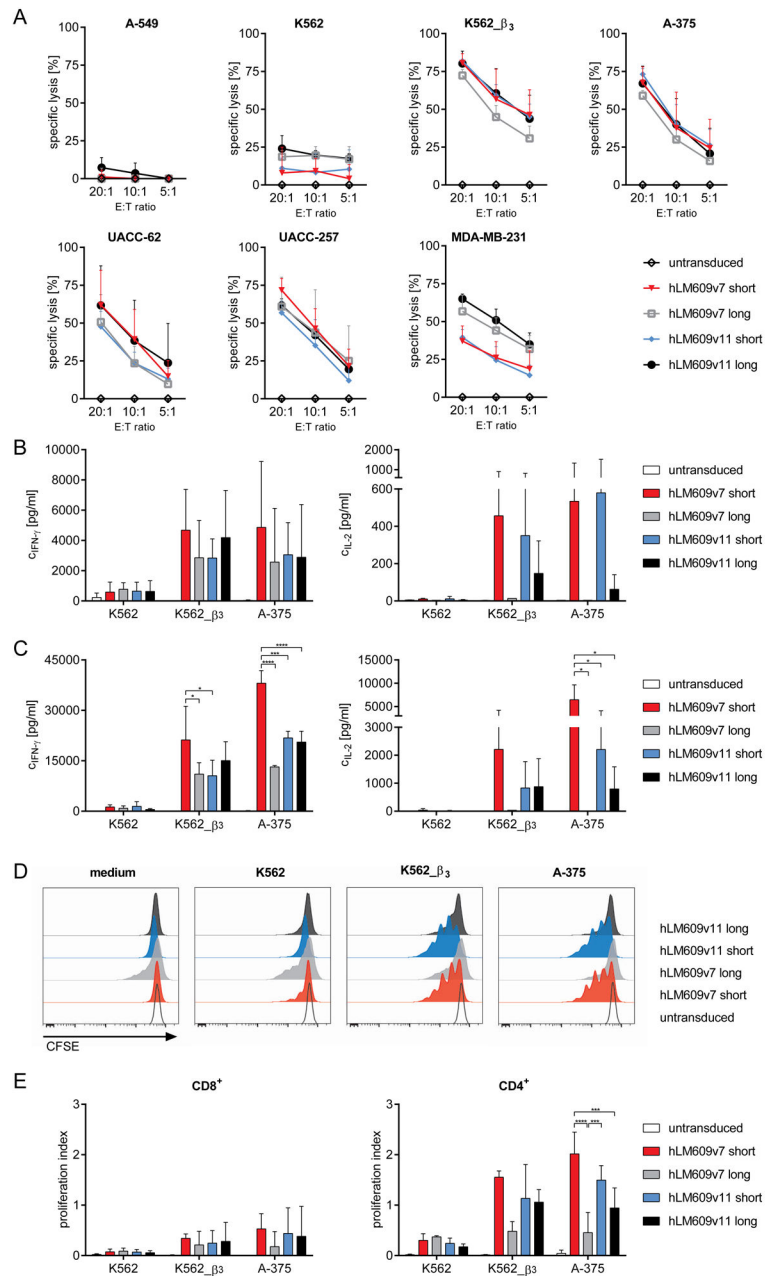


Figure 3. $\alpha_v\beta_3$ -CAR T-cells confer antitumour reactivity *in vitro*.

(A) Specific lysis of ffluc/GFP⁺ tumour cell lines by $\alpha_v\beta_3$ -CAR modified CD8⁺ T-cells after 4 h. Presented is the mean of n = 3 experiments, error bars depict SD. (B) Concentration of IFN- γ and IL-2 in supernatants after 22 h co-culture of CAR modified or untransduced CD8⁺ or (C) CD4⁺ T-cells and tumour cell lines. Presented is the mean of n = 3 experiments, error bars depict SD; only significant differences between the CAR constructs are indicated (* $p < 0.05$, *** $p < 0.001$, **** $p < 0.0001$) (D) Proliferation of CFSE-labelled CD4⁺ T-cells after 72 h co-culture with irradiated tumour cells. The histograms show data from one representative out of n = 3 experiments. (E) Proliferation index of CD8⁺ and CD4⁺

T-cells of n = 3 experiments, error bars depict SD; only significant differences between the CAR constructs are indicated (***) $p < 0.001$, ****) $p < 0.0001$).

Author Manuscript

Author Manuscript

Author Manuscript

Author Manuscript

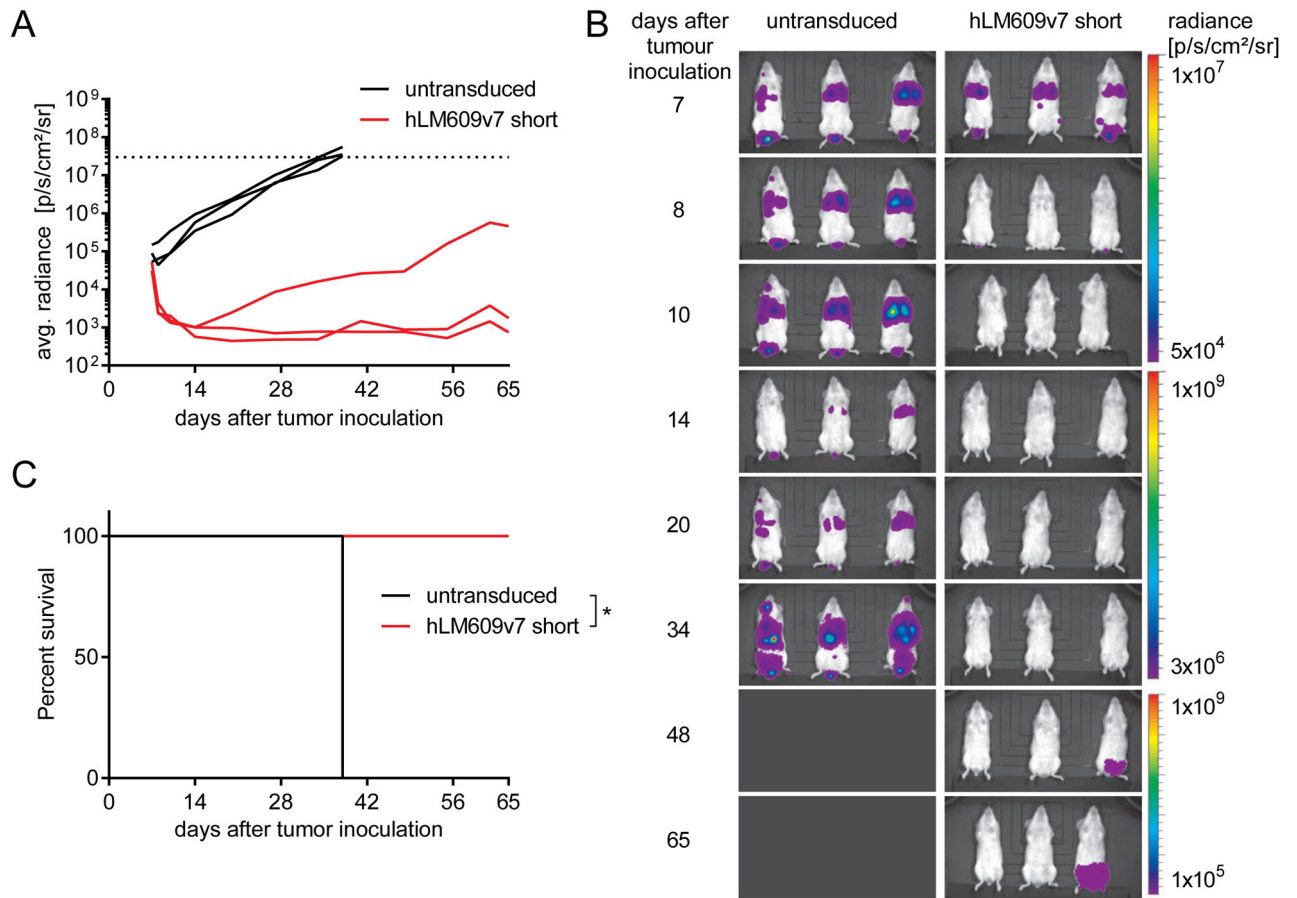


Figure 4. $\alpha_v\beta_3$ -CAR T-cells confer antitumour reactivity *in vivo*.

Mice were injected with 1×10^6 A-375/ffluc_GFP⁺ tumour cells i.v. and treated with a single dose of 5×10^6 T-cells i.v. 7 days later. Groups of $n = 3$ mice either received untransduced or hLM609v7/short $\alpha_v\beta_3$ -CAR T-cells. **(A)** Bioluminescence signal obtained from regions of interests encompassing the entire body of each mouse in the treatment groups. The experiment endpoint was reached at a predefined bioluminescence signal threshold (dotted line). **(B)** Images depict bioluminescence signal intensity and localisation in each of the mice in the treatment groups. **(C)** Kaplan-Meier analysis of survival in groups of mice until the end of the predefined observation period on day 65 after tumour engraftment (* $p < 0.05$)

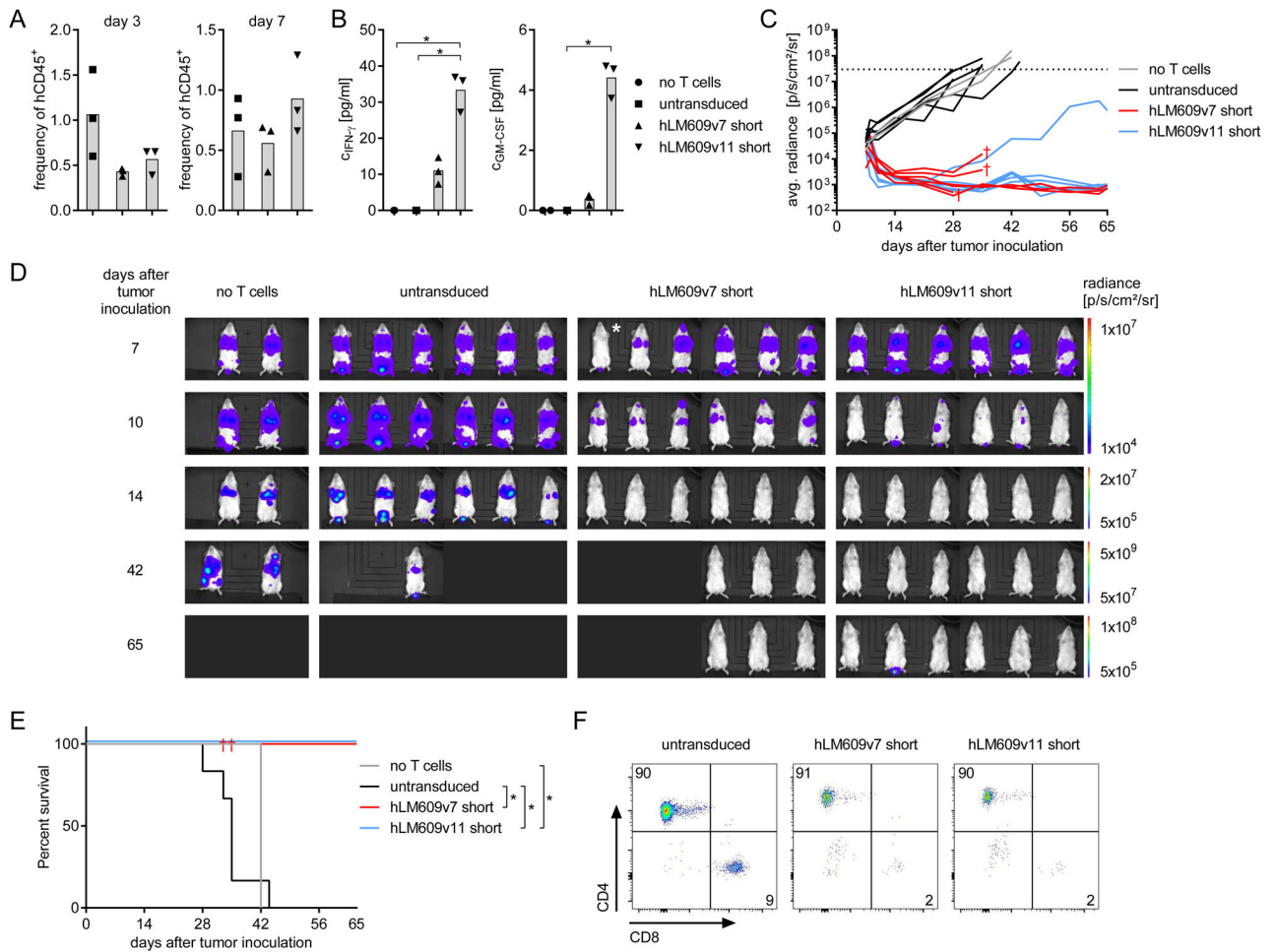


Figure 5. $\alpha_v\beta_3$ -CAR T-cells eliminate metastatic melanoma in a murine xenograft model *in vivo*. Mice were injected with 1×10^6 A-375/ffluc_GFP⁺ tumour cells i.v. and treated with a single dose of 5×10^6 T-cells i.v. 7 days later. Groups of $n = 6$ mice either received untransduced, hLM609v7/short or hLM609v11/short $\alpha_v\beta_3$ -CAR T-cells, and one group of $n = 2$ mice remained untreated. **(A)** Percentage of hCD45⁺ (gated on live 7-AAD⁻ cells) in peripheral blood of mice on day 3 and day 7 after T-cell transfer. **(B)** Serum concentration of IFN- γ and GM-CSF on day 1 after T-cell transfer. **(C)** Progression/ regression of bioluminescence signal obtained from regions of interests encompassing the entire body of each mouse. The experiment endpoint was reached at a predefined signal threshold (dotted line). † indicates that mice were lost to follow-up. **(D)** Bioluminescence images depict signal intensity and localisation generated by A-375/ffluc_GFP⁺ tumour cells in groups of mice that remained untreated or were treated with untransduced, hLM609v7/short or hLM609v11/short $\alpha_v\beta_3$ -CAR T-cells. * Tumour engraftment in this mouse was confirmed using a more sensitive BLI scale. **(E)** Kaplan-Meier analysis of survival in groups of mice until the end of the predefined observation period on day 65 after tumour engraftment (* $p < 0.05$). **(F)** Flow cytometric analysis to detect human T-cells (gated on live 7-AAD⁻ and hCD45⁺ cells) in the bone marrow of mice at the experiment endpoint.